Supplementary Material

Enhanced lignin hydrogenolysis by *in-situ* hydrogen supply through methanol-water aqueous phase reforming over CoTi@biochar catalyst

Tao Yin, Zhaoyuan Huang, Bowen Luo, Zhipeng Tian,* Chao Wang, Jianping Liu, Ying Chen, Riyang Shu*

[a]*Guangdong Provincial Key Laboratory of Functional Soft Condensed Matter, School of Materials and Energy, Guangdong University of Technology, Guangzhou 510006, PR China*

Corresponding author: tianzhipeng@gdut.edu.cn (Zhipeng Tian); shuriyang@gdut.edu.cn (Riyang Shu).

Table S1 Assignment of main ^{13}C-^{1}H cross-signals in the HSQC spectra of the lignin depolymerization non-volatile products.

Catalyst	δ_C/δ_H/ppm	Assignment
-OCH_3	56.0/3.8	Methoxy structure on benzene ring
Aα	71.6/4.7	C_α-H_α in the structure of β-O-4
Aβ	80.5/4.4 & 83.9/4.3	C_β-H_β in the structure of β-O-4 connecting the G units
Aγ	60.4/3.6	C_γ-H_γ in the structure of β-O-4
Aγ′	63.0/3.8-4.10	C_γ-H_γ in the structure of the acetylated β-O-4
Bα	85.4/4.6	C_α-H_α of β-β in resinoid alcohol
Bβ	53.5/3.07	C_β–H_β of β-β in resinoid alcohol
Bγ	72.9/3.7	C_γ–H_γ of β-β in resinoid alcohol
Cα	87.5/5.4	C_α-H_α in phenylcoumarin
Cβ	49.8/3.6	C_β–H_β in phenylcoumarin
Cγ	62.9/3.6	C_γ–H_γ in phenylcoumarin
D	60.6/4.0	pinacol
G2	112.6/6.8	C_2-H_2 in guaiacyl (G)
G5	115.6/6.7	C_5-H_5 in guaiacyl (G)
G6	121.1/6.5	C_6-H_6 in guaiacyl (G)
FA2	110.3/7.2	C_2-H_2 in the structure of ferulic acid esters
FA6	124.2/6.9	C_6-H_6 in the structure of ferulic acid esters
PCE2,6	128.7/7.2	$C_{2,6}$-$H_{2,6}$ in p-coumarate structure
H2,6	125.8/6.9	$C_{2,6}$-$H_{2,6}$ in p-hydroxyphenyl structure
X5	62.8/3.3	C_5-H_5 in β-D-pyranopyranoside

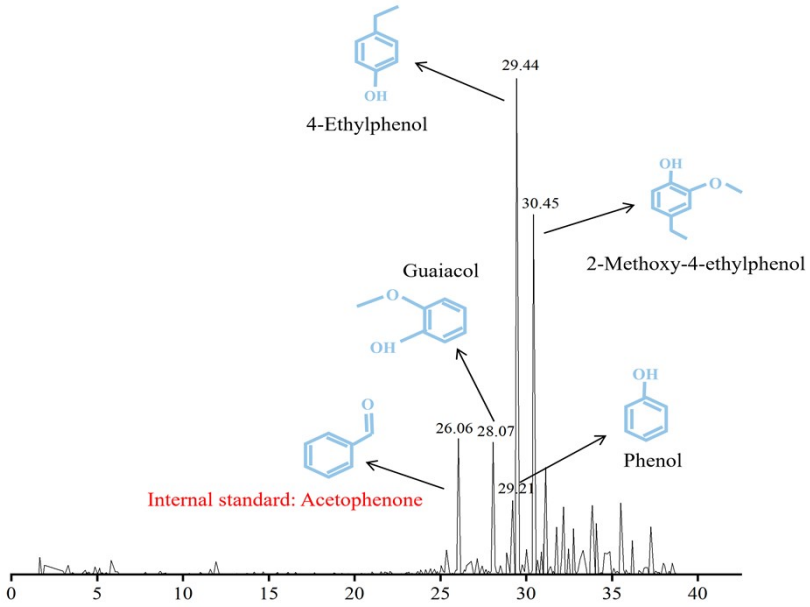

Fig. S1. GC-MS chromatogram of the aromatic monomers from lignin depolymerization catalyzed by CoTi@BC catalyst.

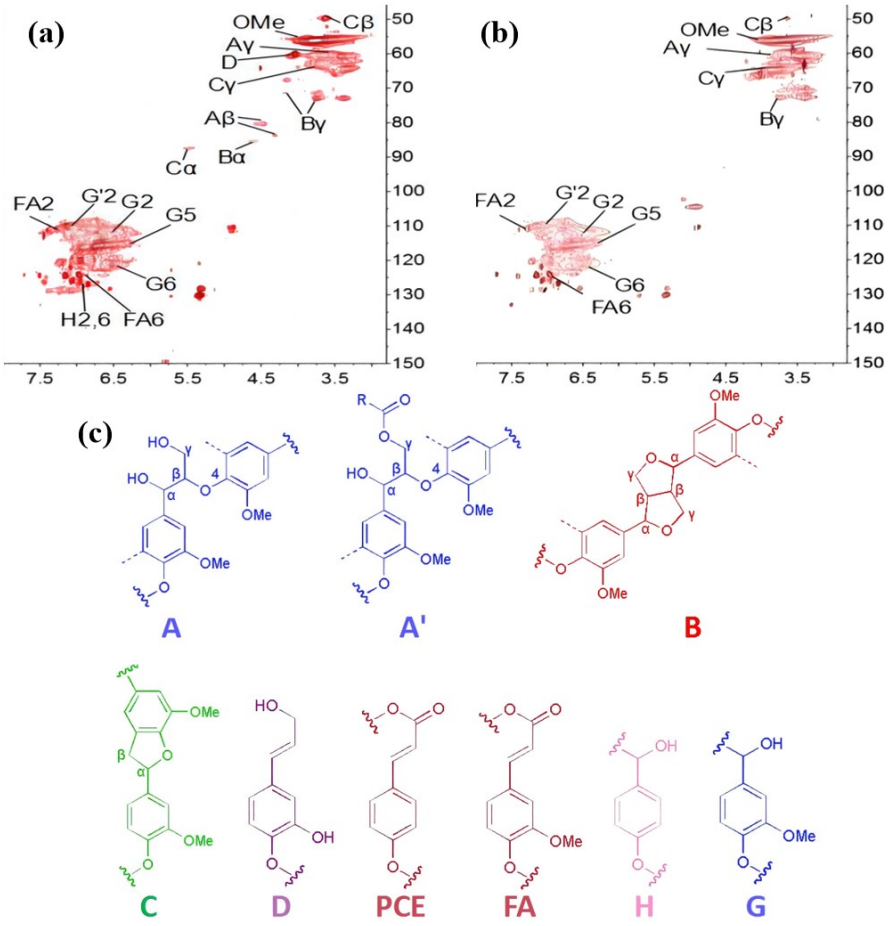

Fig. S2. 2D-HSQC NMR spectra of (a) enzymatic lignin, (b) after hydrogenolysis of enzymatic lignin with CoTi@BC catalysts and (c) the classical bonding patterns.

Note: Symbol attribution is detailed in Table S1 (assignment of main ^{13}C-^{1}H cross-signals in the HSQC spectra of the enzymatic lignin).

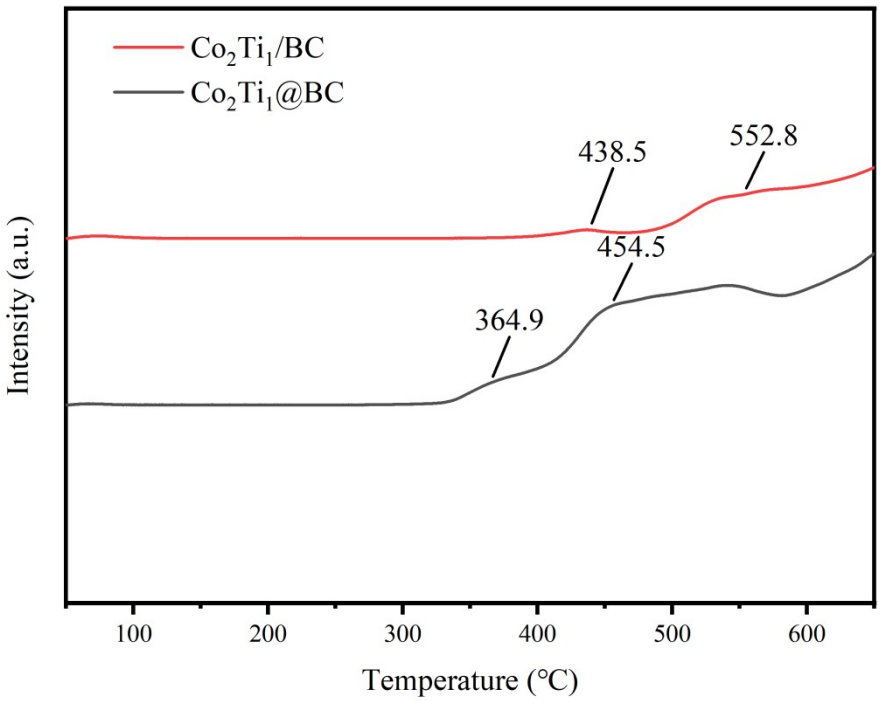

Fig. S3. The H_2-TPD profiles of Co_2Ti_1@BC and Co_2Ti_1/BC catalysts.

Table S2. The H_2-TPD profiles of Co_2Ti_1@BC and Co_2Ti_1/BC catalysts.

Catalysts	Hydrogen adsorption amount (mmol/g)[a]	Sample mass (g)	Co loading[b] (wt.%)	Co dispersion (%)
Co_2Ti_1@BC	0.455	0.060g	9.92	8.9
Co_2Ti_1/BC	0.102	0.060g	10.06	2.0

[a] Data derived from H_2-TPD characterization.

[b] Data derived from ICP-AES results.

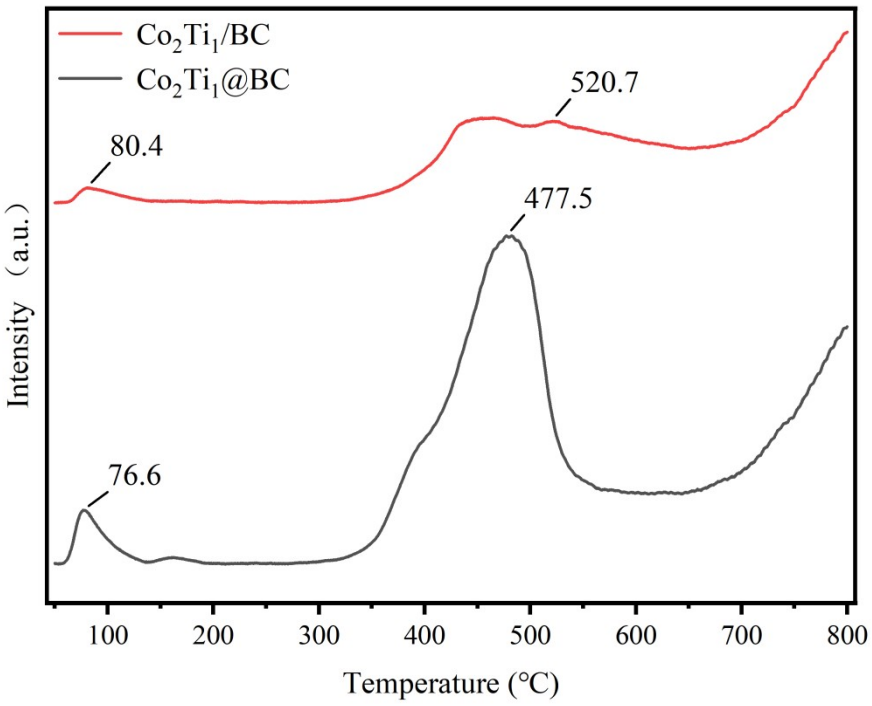

Fig. S4. The NH_3-TPD profiles of Co_2Ti_1@BC and Co_2Ti_1/BC catalysts.

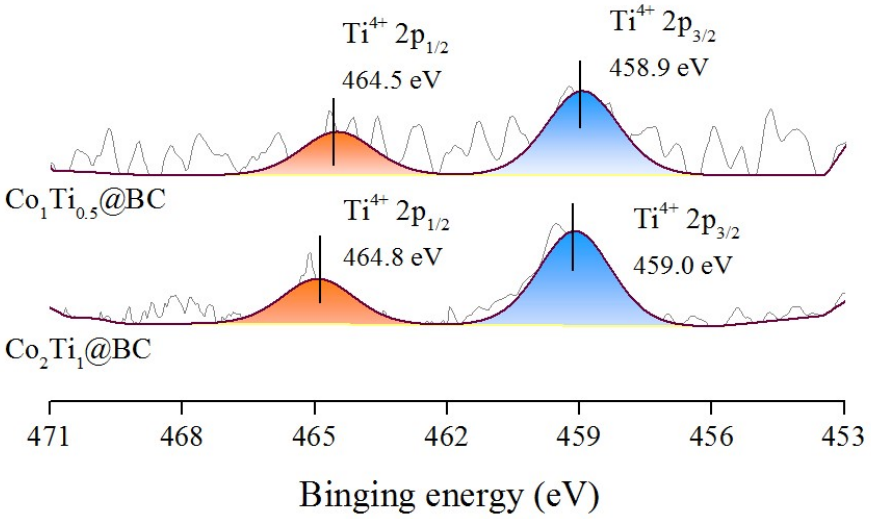

Fig. S5. The deconvoluted XPS spectra of Ti in the different Co-based catalysts.

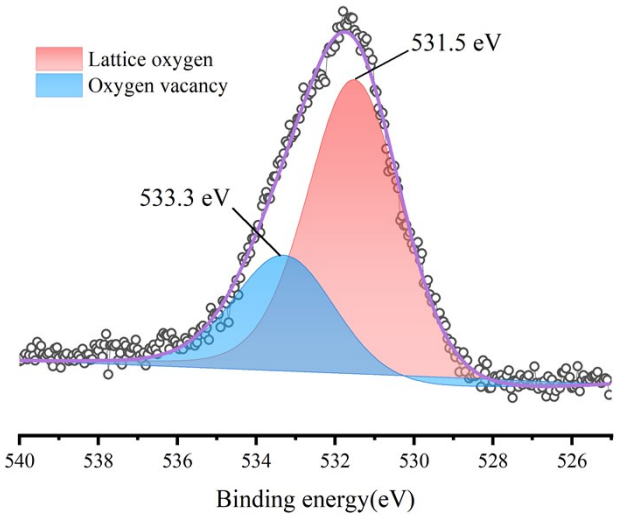

Fig. S6. The deconvoluted XPS O 1s spectra of Co_2Ti_1@BC catalyst.

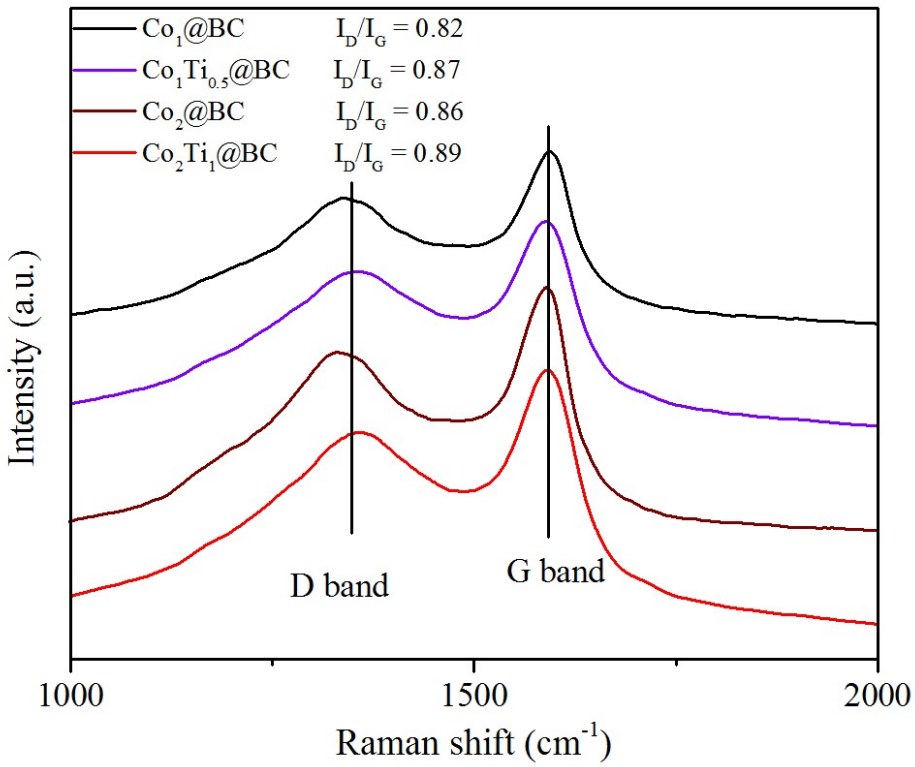

Fig. S7. The Raman spectra of different Co-based catalysts.

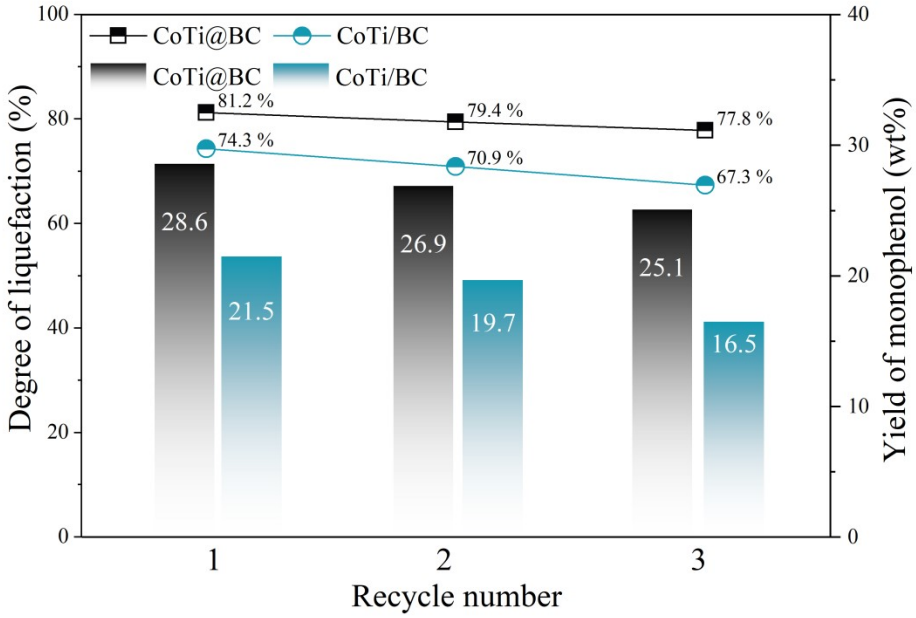

Fig. S8. The reusability of Co_2Ti_1@BC and Co_2Ti_1/BC catalysts.

Reaction conditions: 0.5 g enzymatic lignin, 0.2 g catalyst, 20 mL methanol-water solution, 2 MPa Ar, 250 °C, 4 hours.

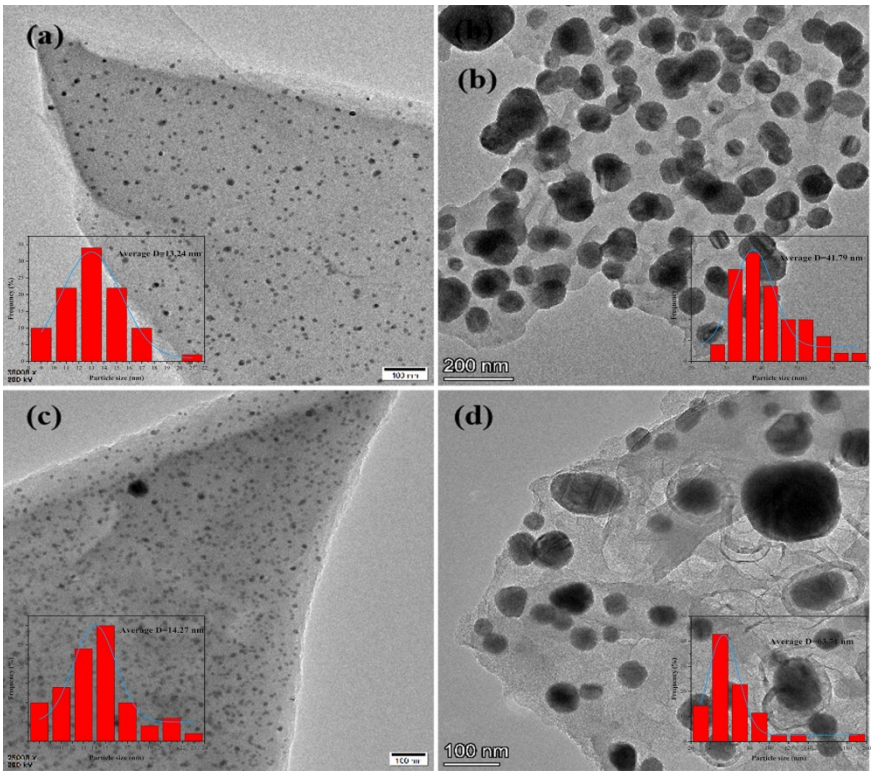

Fig. S9. TEM image of different Co-based catalysts. (a) Co_2Ti_1@BC, (b) Co_2Ti_1/BC, (c) recycled Co_2Ti_1@BC and (d) recycled Co_2Ti_1/BC catalyst

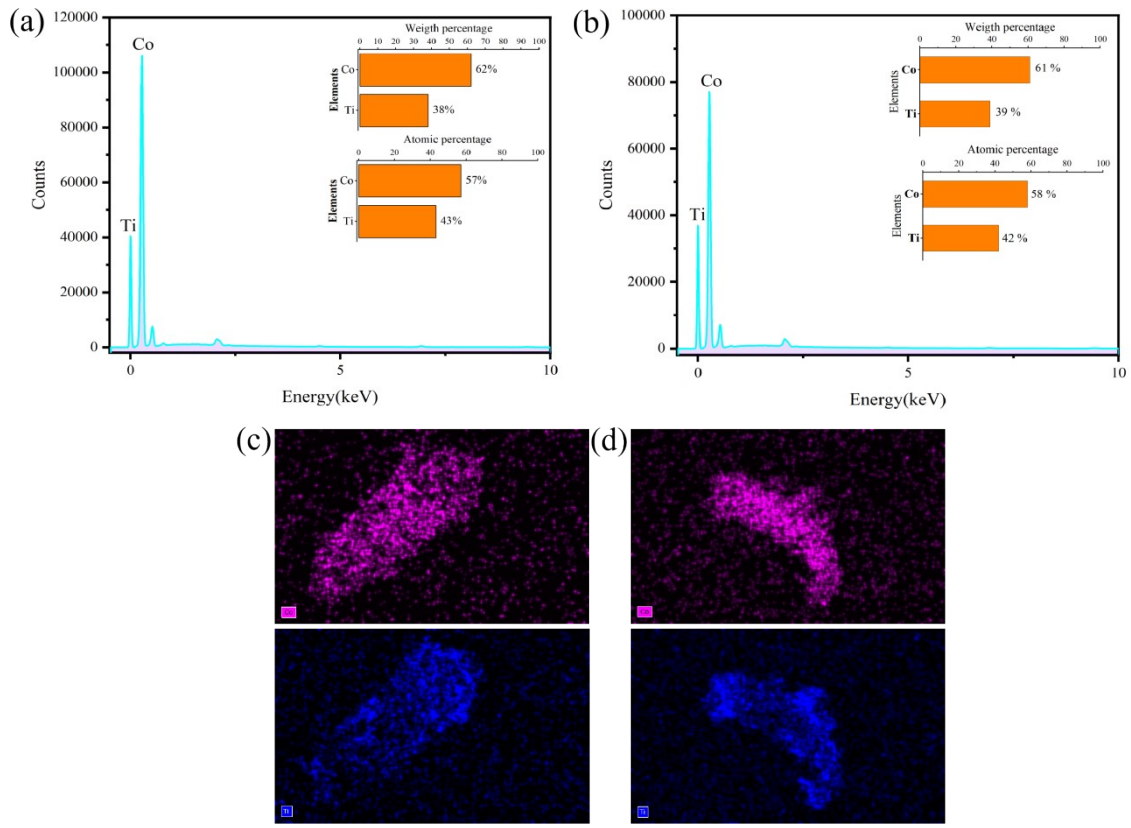

Fig. S10. The SEM-EDS analysis and elemental mapping of the (a) (c) fresh and (b) (d) used Co_2Ti_1@BC catalysts.

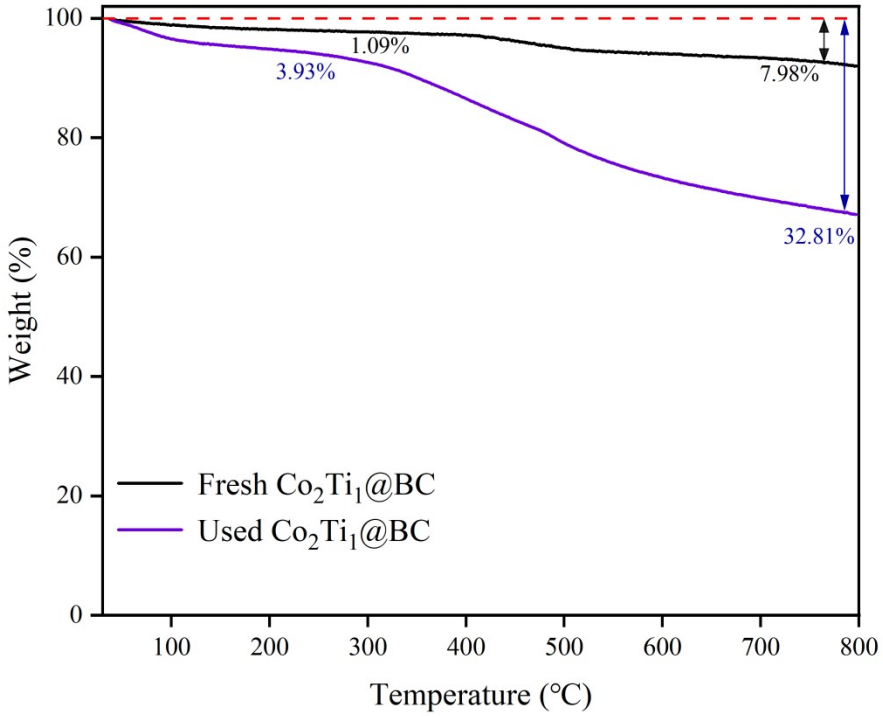

Fig. S11. TGA profiles of the fresh Co_2Ti_1@BC and used Co_2Ti_1@BC catalysts.

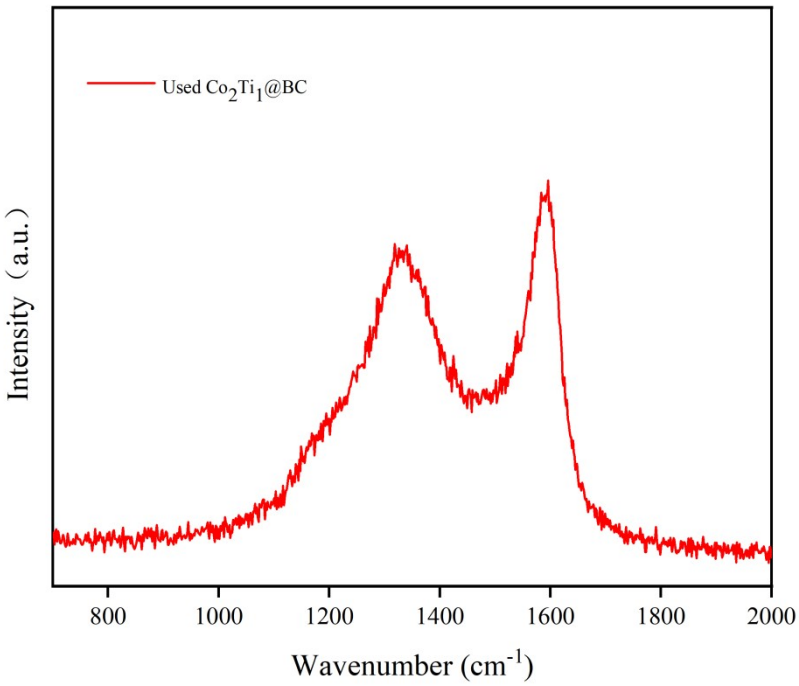

Fig. S12. Raman spectra of used Co_2Ti_1@BC catalysts.